Schweizerische Eidgenossenschaft
Confédération suisse
Confederazione Svizzera
Confederaziun svizra

Department of the Environment, Transport, Energy and Communication DETEC

Swiss Federal Office of Energy SFOE
Energy Research

Final report

Impacts of Atmospheric and Wake Turbulence on Wind Turbine Fatigue Loading

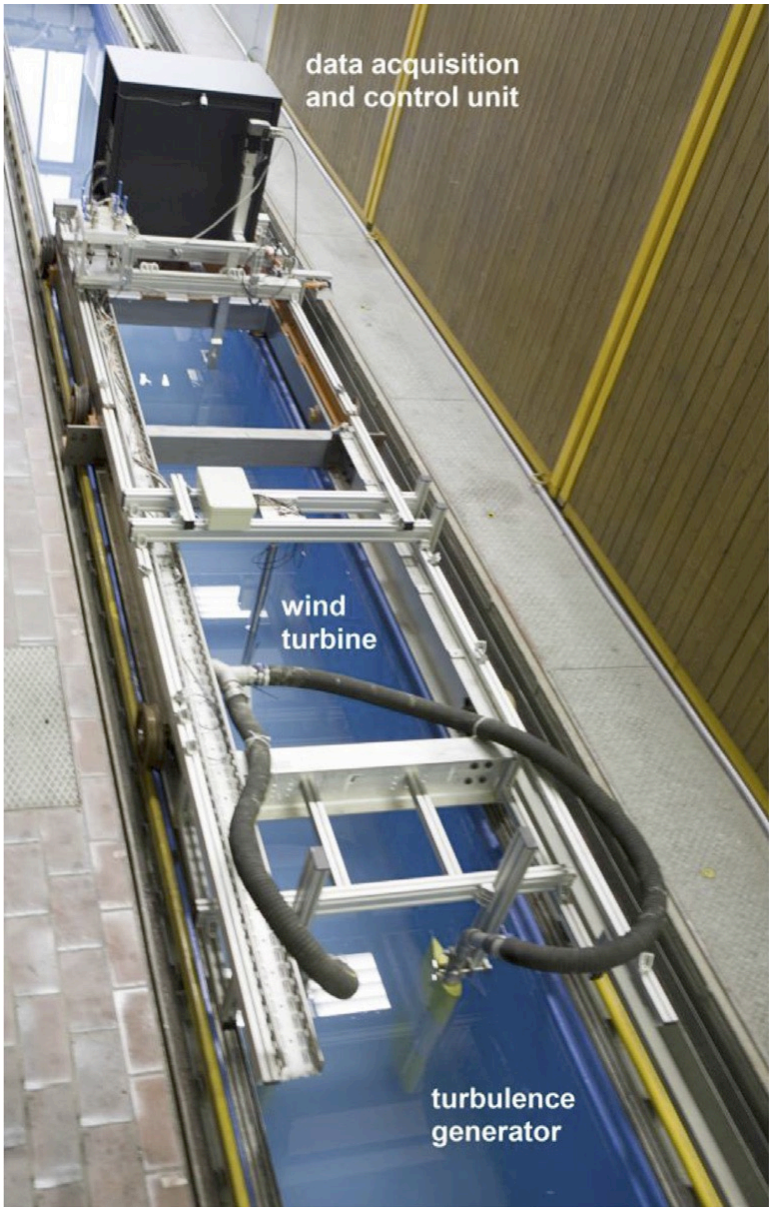

LEC
Laboratory for Energy Conversion

Date: 31 August 2017
Town: Zürich

Publisher:
Swiss Federal Office of Energy SFOE
Forschungsprogramm Windenergie
CH-3003 Bern
www.bfe.admin.ch

Agent:
Laboratory for Energy Conversion
ETH Zürich
Sonneggstrasse 3
CH-8092 Zürich
www.LEC.ethz.ch

Author:
Ndaona Chokani, Laboratory for Energy Conversion, ETH Zürich, chokanin@ethz.ch
Reza Abhari, Laboratory for Energy Conversion, ETH Zürich, abhari@ethz.ch

SFOE head of domain: Katja Maus, katja.maus@bfe.admin.ch
SFOE programme manager: Lionel Perret, lionel.perret@Planair.ch
SFOE contract number: SI/501107-01

Swiss Federal Office of Energy SFOE
Mühlestrasse 4, CH-3063 Ittigen; postal address: CH-3003 Bern
Phone +41 58 462 56 11 · Fax +41 58 463 25 00 · contact@bfe.admin.ch · www.bfe.admin.ch

Contents

List of abbreviations

D	diameter, proportionality constant
DC	direct-current
EDM	electrical discharge machining
ES2050	Energy Strategy 2050
HF	high-frequency
IPC	individual pitch control
Li-Po	lithium-polymer
PCB	printed-circuit-board
PWM	pulse-width-modulated
P_{IPC}	corrective pitch adjustment
P_0	collective pitch angle
R	rotor radius
SSI	synchronous serial interface
TSR	tip speed ratio
U	streamwise velocity
WEST	wind turbine test
x	axial displacement of blade tip
y	horizontal position of traverse
z	vertical position of traverse

φ	rotor tilt angle
θ	azimuthal position of rotor
$\dot{\theta}$	rotational speed of the turbine

Zusammenfassung

Für die in der Schweiz installierten Windenergieanlagen wurde ein skaliertes Modell moderner, drehzahlvariabler Multimegawatt-Turbinen mit variabler Pitchregelung entwickelt, welches in der ETH WEST Facility konstruiert, gefertigt und installiert wurde. Im Gegensatz zu früheren Arbeiten, die in erster Linie Simulationen zur Untersuchung der unabhängigen Pitchregelung verwendet haben, präsentiert dieses Projekt die erste experimentelle Untersuchung der unabhängigen Pitchregelung mit einer Subskalenmodell-Windturbinentestanlage. Nach Wissen der Autoren ist dieses Projekt die erste experimentelle Untersuchung der unabhängigen Pitchregelung mit einer Subskalenmodell-Windturbinentestanlage. Es wird gezeigt, dass eine unabhängige Pitchregelung, die auf einer sinusförmigen Neigung der Rotorblätter basiert und welche an die Phase der Rotordrehung gekoppelt ist, je nach Gierwinkel der Turbine eine Leistungssteigerung von 10-16% ergeben kann. Die Leistungserhöhung tritt auf, weil die sinusförmige Neigung der Rotorblätter die durch die Rotorneigung induzierten Geschwindigkeitsschwankungen kompensiert. Diese Rotorneigung ist charakteristisch für modern Multimegawatt-Turbinen. Da die erfolgreiche Entwicklung der unabhängigen Pitchregelung für das Subskalenmodell eine gewaltige Herausforderung war, waren die Messungen mit erhöhten Turbulenzen begrenzt. Trotzdem wurde beobachtet, dass bei erhöhter Turbulenz die Nachlaufströmung asymmetrisch ist, was der Rotation des Nachlaufströmung zugeschrieben werden kann. In laufenden Arbeiten werden die Auswirkungen von erhöhten Turbulenzen auf die Belastung experimentell quantifiziert.

Résumé

Un modèle à l'échelle de turbines multi-mégawatt modernes, à vitesse variable et à maîtrise en tangage variable représentatif des éoliennes installées en Suisse a été conçu, fabriqué et installé dans l'ETH WEST facility. Contrairement aux travaux antérieurs qui ont utilisé principalement des simulations pour étudier une maîtrise en tangage indépendante, ce projet présente la première étude expérimentale de maîtrise en tangage indépendante avec une installation de test de turbine éolienne à sous-échelle. À la connaissance des auteurs, ce projet est la première étude expérimentale de maîtrise en tangage indépendante avec une installation de test de turbine à vent sous-échelle. Il est démontré que la maîtrise en tangage indépendante basée sur le tangage sinusoïdal qui est verrouillé à la phase de rotation du rotor peut produire une augmentation de puissance entre 10-16% selon l'angle de lacet de la turbine. L'augmentation de puissance se produit car le tangage sinusoïdal compense les variations de vitesse induites par l'inclinaison du rotor. Cette inclinaison du rotor est une caractéristique de turbines multi-mégawatt modernes. Comme le développement à success de la maîtrise en tangage indépendante pour le modèle de sous-échelle était un redoutable défi, les mesures avec une turbulence élevée étaient limitées. Néanmoins, on a observé que, avec une turbulence élevée, le sillage est asymétrique, et cette asymétrie est attribuée à la rotation du sillage. Dans les travaux en cours, l'impact de la turbulence élevée sur les charges sera quantifié expérimentalement.

Summary

A scaled-model of modern, variable-speed, variable-pitch-control, multi-megawatt turbines that is representative of wind turbines installed in Switzerland has been designed, manufactured and installed in the ETH WEST Facility. In contrast to prior works that have used primarily simulations to investigate independent pitch control, this project presents the first experimental investigation of independent pitch control with a sub-scale model wind-turbine test facility. To the knowledge of the authors, this project is the first experimental investigation of independent pitch control with a sub-scale model wind-turbine test facility. It is demonstrated that independent pitch control based on sinusoidal pitching that is locked to the phase of the rotor rotation can yield power increases between 10-16% depending on turbine’s yaw angle. The power increase occurs because sinusoidal pitching compensates for the velocity variations induced by rotor tilt; this rotor tilt is a charcaterisitc of modern,

multi-megawatt turbines. As the successful development of the independent pitch control for the sub-scale model was a formidable challenge, the measurements with elevated turbulence were limited. Nevertheless, it was observed that with elevated turbulence the wake is asymmetric, and this asymmetry is attributed to rotation of the wake. In ongoing work, the impact of elevated turbulence on the loads will be experimentally quantified.

Appendix

Appendix

1. Introduction

1.1 Motivation

Switzerland's Energy Strategy 2050 (ES2050) is an outcome of the Swiss parliament's decision to initiate the phase out of nuclear power by 2050 in reaction to the Fukushima nuclear accident. Although the Swiss population rejected a proposal to shut down all Swiss nuclear power plants by 2029 in a recent referendum, nevertheless the Swiss parliament maintains its position of gradually phasing out nuclear power over next three decades. This decision has far-reaching consequences for Switzerland's energy sector, as 38% of Switzerland's electricity production comes from nuclear power. In ES2050, the Swiss Federal Office of Energy proposes, on the generation side, new hydropower plants and new renewable power plants (such as wind farms and photovoltaic installations), and on the demand side, increased energy efficiency, as measures to compensate for the decommissioning of nuclear power. Within the framework of ES2050, it is evident that wind-generated electricity shall comprise a significant portion of renewables in the future energy mix that is required to meet ES2050.

However, as the topography in Switzerland is characterised as a complex terrain, the freestream turbulence levels are elevated compared to the turbulence levels in flat terrain. These elevated turbulence levels have an impact on the evolution of the wakes, that is the low-speed region downstream of a wind turbine. As the interaction of wind turbine wakes with downstream turbines results in up to 30-40% losses in power production, there has been substantial effort to develop both semi-empirical wake models and advanced wind simulation tools. These models and tools are used to assess the optimised placement of wind turbines. Significantly less attention has focused on the fact that there are higher fatigue loads on wind turbines operating in wakes. These higher loads lead to a reduced operational lifetime of wind turbines' components. The higher loads also result in significantly higher maintenance costs, which currently account for 10-20% of the total cost of wind-generated electricity.

Furthermore, as large-scale wind is a relatively new addition to Switzerland's energy sector, the new wind farms in Switzerland that are required to accomplish the goals of ES2050 shall be equipped with modern multi-megawatt wind turbines that, as described in the next section, are of a variable-speed, variable pitch design. It is therefore of paramount interest to understand the operation of modern multi-megawatt wind turbines in the context of Switzerland's specific environment.

1.2 Research Objectives

Thus, the overall goal of this project is to quantify the effects of elevated turbulence levels on the loads on wind turbines. In this project, in order to experimentally address the impact of elevated turbulence levels on turbine loading, the following tasks will be undertaken:

– Design, manufacture and installation of scaled-multi-megawatt wind turbine model.

– Design, manufacture and integration of independent pitch control mechanism in model.

– Measurements of wake evolution as a function of freestream turbulence levels.

– Measurements of the turbine performance with independent pitch control.

Thus, this final report is organised as follows: first, the operation of modern multi-megawatt wind turbines is described; then, the design of the scaled-model turbine with independent pitch control is described; the ETH Wind Turbine Test Facility in which the model is tested is described; then, the results of experiments are reported; and, finally, the report concludes with summary remarks.

2. Operation of modern multi-megawatt wind turbines

2.1 Modes of turbine operation

The operation of wind turbines can be well described from the wind turbine's power curve, Figure 1. In 'Region 1,' at the wind speeds are below the cut-in wind speed, the wind turbine is not operated, and no power is generated. In 'Region 2,' where the wind speeds are between the cut-in and rated wind speeds, the wind turbine is operated. As the available wind power increases in proportion to the cube of the wind speed, there is a commensurate increase in the generated power of the wind turbine with increase in wind speed. At the rated wind speed, the generated power equals the rated power of the generator, and thus in 'Region 3,' where the wind speeds are between the rated wind speed and the cut-out wind speed, the generated power is constant. Above the cut-out wind speed, the wind turbine is shutdown, in order to preserve the structural integrity of the wind turbine, and therefore no power is generated.

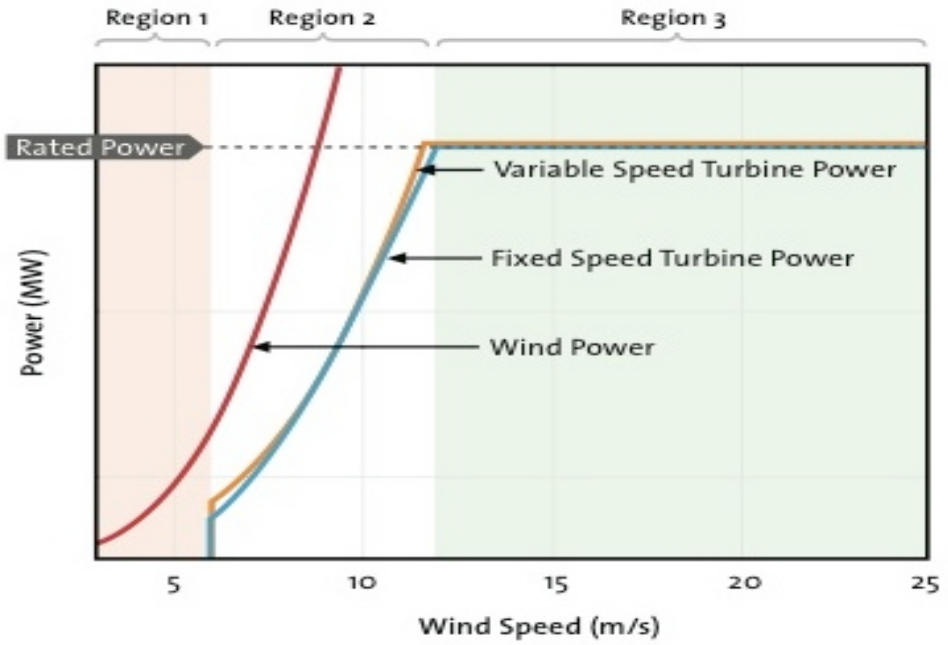

Figure 1: Operating regions of modern wind turbines

2.2 Pitch control on wind turbines

In 'Region 2' of the turbine's operation it is desirable to operate the wind turbine at maximum aerodynamic efficiency, Figure 2. For a given wind turbine design as the maximum aerodynamic efficiency is obtained at a specific tip-speed-ratio (that is ratio of blade tip speed to wind speed), in 'Region 2' the maximum aerodynamic efficiency can be attained if also the rotational speed of the wind turbine is changed in proportion to the wind speed. Thus, modern wind turbines have a variable

rotational speed, commonly termed variable speed, in contrast to legacy wind turbines, which have a fixed speed. For given wind conditions a variable-speed wind turbine can have up to 5% more annual energy yield than a fixed-speed wind turbine in the same wind conditions. Above the rated wind speed, when the wind speed is between the rated and cut-out wind speeds, constant power must be generated. This is accomplished by pitching the blades, Figure 2. In the case that the wind speed increases the blades are pitched towards 'fine,' and in the case that the wind speed decreases the blades are pitched towards 'feather.' Pitch control is thus necessary for a modern wind turbine to operate in 'Region 3.' Furthermore, in 'Region 2,' as the inertia of the wind turbine rotor is substantially larger than the inertia of a single wind turbine blade, for small changes in wind speed, pitch control is a more effective means of maintaining the maximum aerodynamic efficiency than variable-speed operation. Thus, blade pitching is also used, in 'Region 2,' to maintain maximum aerodynamic efficiency, when the wind speed is between cut-in and rated wind speeds. Variable-pitch wind turbines thus dominate the current state-of-the art modern multi-megawatt wind turbines. These variable-pitch wind turbines dynamically and independently adjust the pitch position of each blade during revolution of the rotor. However, in practice, variable pitch control is typically deployed in the form of "collective" pitching which enforces identical pitch positions for all three blades, typically as a means of curtailing rotational speed and power production at wind speeds above the rated wind speed. Strategies for independent pitch control have received considerable attention in the literature, with reviews in [1-3]. In previous studies, independent pitch control has been proposed as a means of mitigating the unsteady loads caused by wind shear, blade-tower-interaction, yaw / tilt and turbulence [3], as well as gravitational loads acting on the blades [4] with a predominant focus on once-per-revolution, 1P, excitations. The secondary effects of phase delay [5] and higher-order harmonics [6] have also received consideration, including 3P excitations typically associated with blade-tower-interactions for a three-bladed rotor. Previous studies have relied primarily upon simulations to validate the proposed pitch algorithms. To the knowledge of the authors, this project is the first experimental investigation of independent pitch control with a sub-scale model wind-turbine test facility.

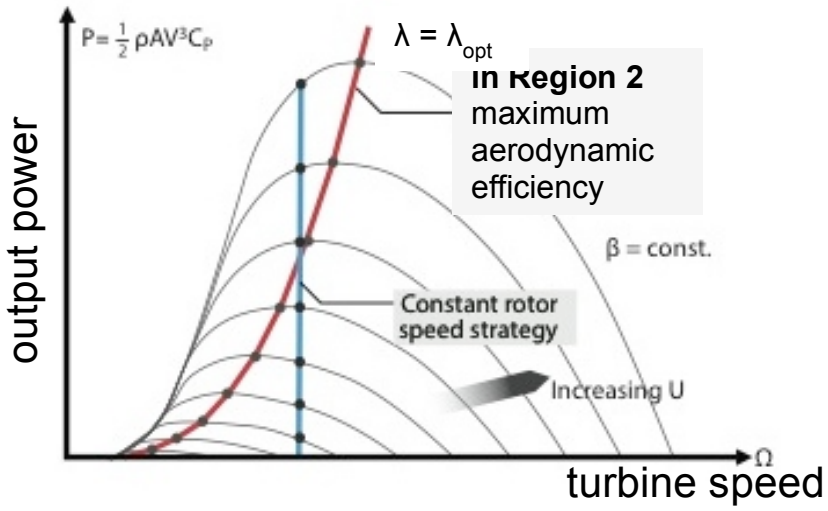

(a)

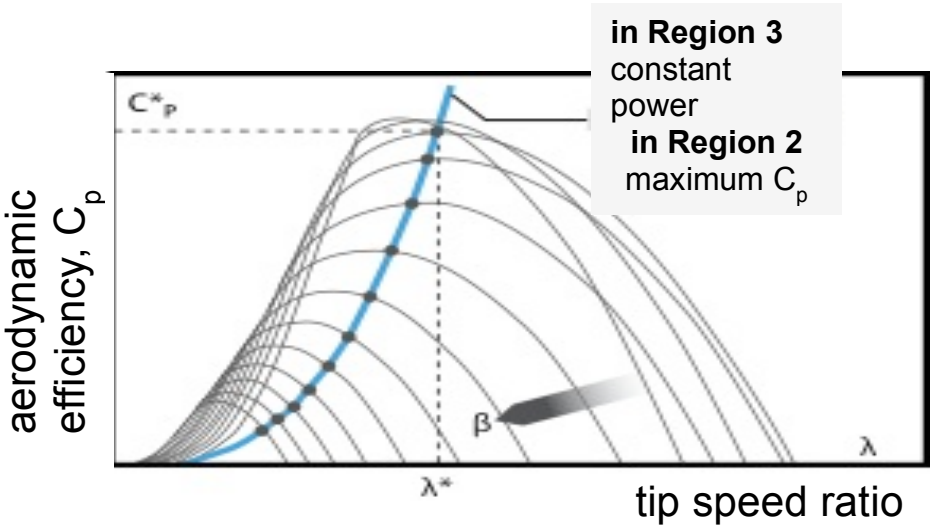

(b)

Figure 2: (a) effect of wind speed on turbine power; and (b) effect of blade pitch on turbine power

3. Design of independent pitch control system (IPC)

3.1 Selection of inpedendent pitch control mechanism

The drivetrain of the model turbine, which is installed within the nacelle, Figure 3, is comprised of a 4-pole electric motor that is connected across a dual-bearing configuration to the wind turbine rotor through a turbine drive shaft; the power train is described in detail in [7]. A strain gauge configuration within the driveshaft, which is between the rotor and the dual-bearing configuration, ensures direct measurement of the rotor torque without parasitic losses.

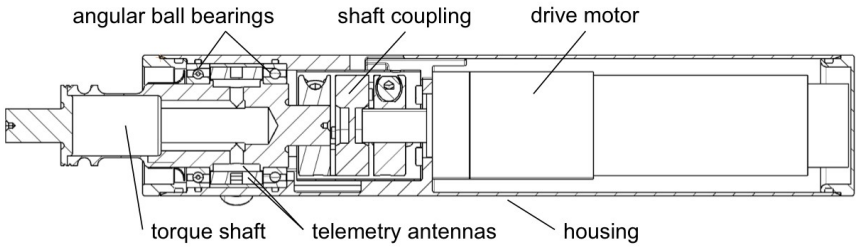

Figure 3: Cross-sectional view of mechanical housing.

Thus, it was necessary to design and build an individual pitch control mechanism that could be integrated into this existing model with no increase in the overall size of the model. Several different candidate configurations, summarised in the Pugh chart shown in Table 1, were assessed for the individual pitch control system.

	precision of angle control	complexity/size	influence of turbine torque	pitch angle up to 90deg.	pitch rate up to 130deg./s	sealing	adequate force/torque	adjustable cone angle	telemetry	**sum × weight**
Pneumatic	-2	-1	0	+2	+1	-1	-1	-1	×	**-11**
Hydraulic	-2	-2	0	+2	-2	-2	+2	-1	×	**-3**
Electrical										
Piezo-motor	-2	+2	0	-2	+2	0	-1	+1	√	**-2**
DC-motor	+2	-1	0	+2	+2	0	-1	+1	√	**+12**
Stepper-motor	+2	-2	0	+2	+2	0	-1	0	√	**+7**
Hub magnet	-2	0	0	-2	+2	0	+2	-1	√	**-3**
WT motor energy	+2	+2	-2	-2	+2	+2	+2	-2	×	**+14**
Gear	+2	-2	0	+2	+2	+2	+2	-2	√	**+16**
Linear direct	+1	-1	0	+2	+2	0	+2	-2	√	**+9**
Rotary direct	+2	0	0	+2	+2	0	+2	1	√	**+23**
Weight: 1-3	3	2	1	2	2	3	3	3		**-11**

Table 1: Pugh Chart analysis of candidate pitch control systems

Based on the requirements based on the dynamic scaling (between model and full-scale) of rotor speed, maximum pitch rate, shaft torque and flapwise bending moment at blade root a DC motor integrated into the blade root was found to best meet all requirements.

3.2 Pitch control system developed for model wind turbine

The individual pitch control (IPC) system has been designed to provide dynamic adjustment of the blade pitch positions during revolution of the rotor. Motorised adjustment of the blade pitch positions is achieved with the installation of a brushless direct-current (DC) motor inside the root of each blade. The root of each blade has therefore been enlarged to house the motor, Figure 4.

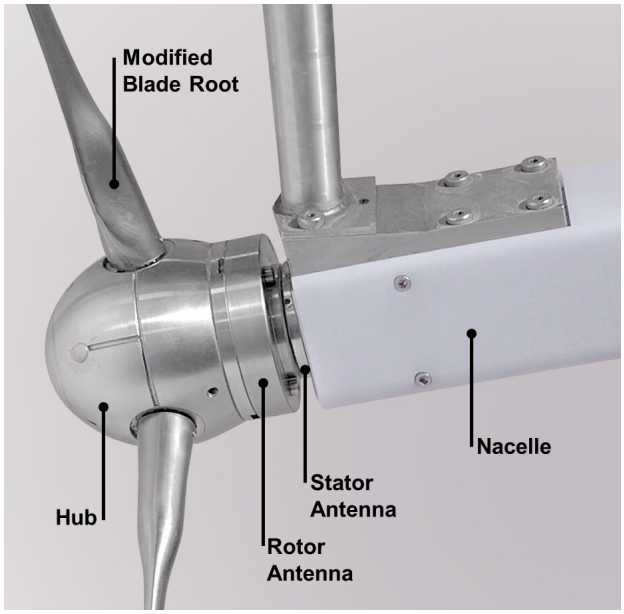

Figure 4: Close-up view of sub-scale wind turbine model, showing the nacelle, rotor with modified blade roots, and rotor-stator antennae.

As the blade root needed to be enlarged, the effect of enlarging the blade root was assessed using our in-house blade element momentum (BEM) code. Analysis of BEM predictions shows that with the enlarged blade root, there is a power reduction of only 2.3% compared to the blade without a modified root. This small reduction occurs because the primary power extraction occurs along the unmodified outboard portion of the blade.

The motor, inside the blade, is connected to a pitching mechanism. A first design, which was assessed to provided sufficient stiffness and strength, was manufactured. However, due to the enlarged blade root, unsteady loads due to vortex shedding resulted in a failure of the pitch mechanism. Specifically, as shown in Figure 5, bending loads caused pins to shear through the gearbox casing. Furthermore, internal componens of the gearbox also failed under the bending loads.

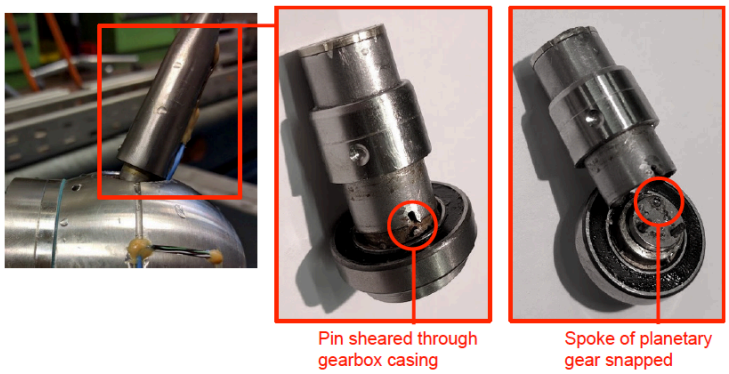

Figure 5: Failure of first-design pitch mechanism system.

In order to address the shortcomings of this first design, the stiffness and strength of the pitch mechanism were reinforced in order to conteract:

– Seizing of the gear train under bending loads.

– Failure of of gearbox under bending loads.

– Low frequency excitation

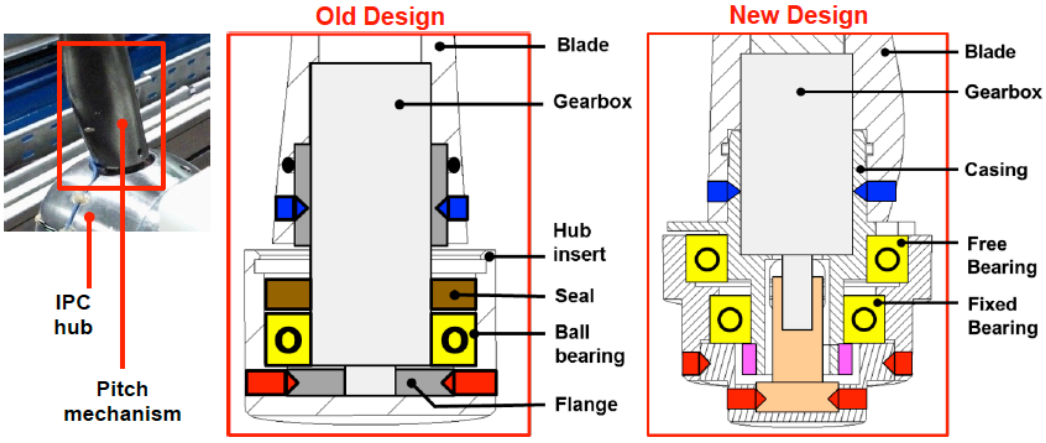

Figure 6: Old and new designs of pitch mechanism system.

As the mechanical failure of the first design was wholly unexpected, this resulted in a substantial delay in the project. This delay due the the the mechanical failure was moreso compounded, as the design of the electronics for the individual pitch control system, described below, also required many novel developments. Thus, as detailed in the Annual Report that was submitted in January 2016, in order to ensure integration of the independent pitch control mechanism in the new model of modern multi-megawatt turbines, Task 1.2, which was originally scheduled for the first quarter of Year 2, was advanced to Year 1. However, the development of the independent pitch control mechanism required several iterations, and thus in order to keep the project on schedule, the first experiments were made in Task 2.3, which was originally scheduled for Year 2, and the experiments of Task 2.1, which was originally scheduled for Year 1 was rescheduled to Year 2. In the Gantt Chart shown in Table 2, the originally proposed schedule is shown in black and the revisions are shown in red.

	Year 1				Year 2				Year 3			
Quarter	**1**	**2**	**3**	**4**	**1**	**2**	**3**	**4**	**1**	**2**	**3**	**4**
Work Package 1												
1.1. Mechanical design and manufacture of scaled-2.5MW-model wind turbine												
1.2. Mechanical design, manufacture and integration of independent pitch control mechanism												
Work Package 2												
2.1. Measurements of wake evolution in elevated turbulence levels												
2.2. Data reduction and analysis												
2.3. Measurements of turbine loads in atmospheric flow turbulence levels												
2.4. Data reduction and analysis												
2.5. Measurements of turbine loads in wake flow turbulence levels												

2.6. Data reduction and analysis												

Table 2: Original project schedule (shown in black) and revised project schedule (shown in red). The revised project schedule was necessary to accommodate the unanticipated mechanical failure and revision in the design of the pitch mechanism that is now working in a reinforced version.

Figure 6 compares the old and new designs of the pitch mechanism. A gearbox, connected to the shaft of the motor, has been installed inside a titanium casing mounted in a duplex steel housing with a preloaded dual ball bearing configuration consisting of one bearing press-fit into the housing and another “free” bearing able to adjust relative to the applied preload. The preload is applied with a titanium nut, which pressures the inner raceways of the bearings for maximum distance between the pressure centres to maximise bending stiffness. The shaft of the gearbox is fastened with a coupling to the housing and the coupling design ensures the transmission of torsional loads, while bending and axial loads are transmitted primarily through the titanium gearbox casing to prevent seizing of the gearbox during operation. A 6-stage spur gearbox (161:1) has been used in the blade pitch mechanism with preloading to reduce clearance between the gearbox stages. The connection between the gearbox shaft and the coupling has been manufactured with electrical discharge machining (EDM) to obtain a high-tolerance (5μm) transitional fit while the coupling is fixed with a press-fit steel pin.

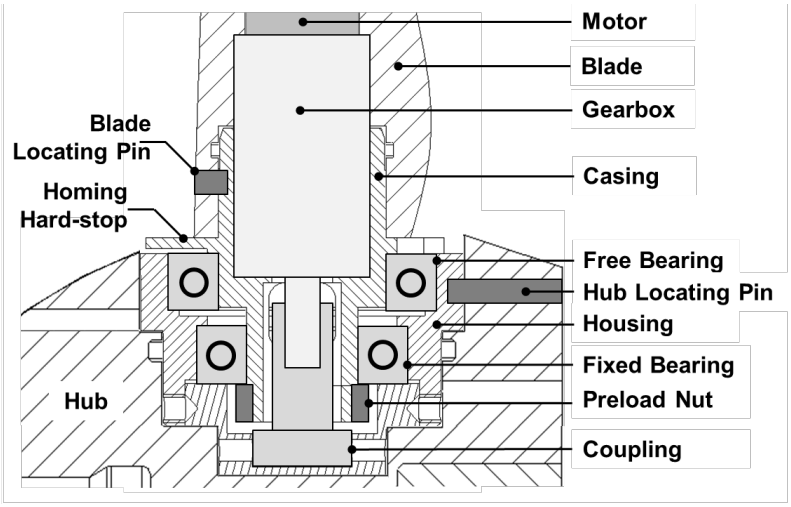

Figure 7: Cross-sectional schematic of pitch mechanism system.

The entire pitch mechanism is positioned within the hub with the aid of a locating pin, while a second locating pin positions the blade. Hard-stops are machined directly onto the housing and gearbox casing, with a precision of 0.1°, Figure 7, allowing the blades to be homed between successive measurements. Camera measurements performed with the entire pitch mechanism assembly confirmed the homing procedure is repeatable within 0.2°, while the total backlash for the pitch mechanism, including connections between the motor, gearbox, coupling and housing, is 1.2°.

Independent positioning of the blades is performed with a control system that consists of manufacturer-supplied controllers, which interface with the motors that are installed inside the blades, together with a custom-built signal transmission system, which sends power, and control signals from a stator antennae on the nacelle to a rotor antennae on the hub, Figure 8.

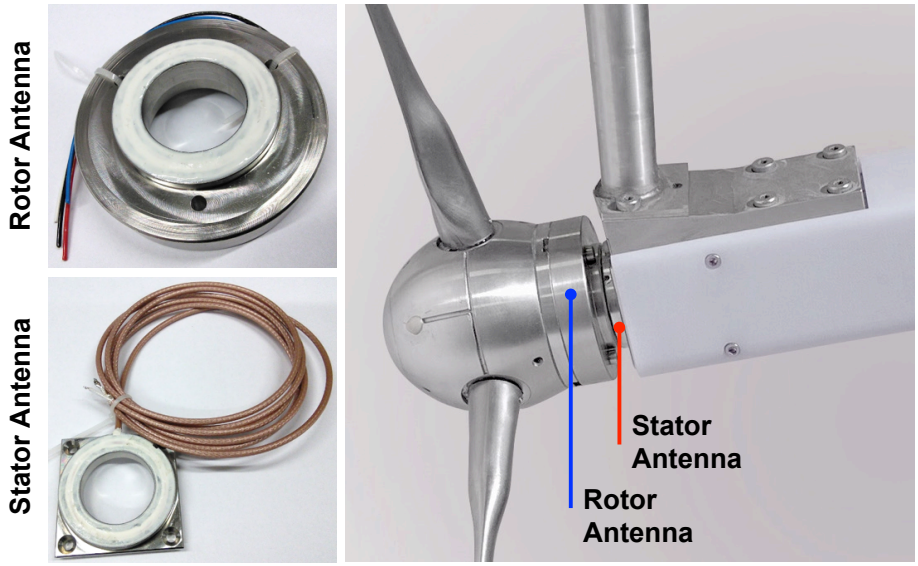

Figure 8: Rotor and stator antennae using for power transmission and control

Inductive power transmission between the antennae coils is driven with a 6.78MHz / 50V peak-to-peak alternating current on the stator side, which is converted into direct current with a high-frequency (HF) generator on the rotor side. Transmission of the power can be “chopped” with a switch on the stator side, at a maximum frequency of 5 kHz, creating a falling edge in power transmission, which can be detected on the rotor side. A pulse-train of falling edges acts as the control signal, with the period between pulses encoding the commanded blade pitch position for each blade, with an uncertainty of 0.14° in the inductive pulse transmission. A printed-circuit-board (PCB) on the rotor side reads the period between pulses and produces three separate pulse-width-modulated (PWM) signals at a frequency of 1kHz – one for each motion controller / blade motor – which results in a further uncertainty of 0.2° in the generation and reading of the PWM signals. Each blade motor includes an absolute magnetic encoder, which connects to the motion controller using a Synchronous Serial Interface (SSI). The uncertainty in the SSI interface is reduced to 0.01° by the gear ratio of 161:1 resulting in a negligible contribution to the overall uncertainty in the pitch position of a blade. The pitch position of each blade can thus be updated at a frequency of 200 Hz, which allows the pitch position of each blade to be updated 30-35 times per revolution depending on the operating point, with an estimated total uncertainty of 0.24° in the commanded blade pitch position. Further camera testing indicated a pitching rate of 1°/7microseconds which equates to 1° of blade pitching for approximately 15° of rotor revolution at the design TSR. The power consumption of the blade pitch motors and on-board control electronics reaches approximately 10W during testing while only approximately 3W can be supplied by inductive power transmission between the antennae, with a 0.5mm spacing between the coils. A further 7W is thus supplied by a lithium-polymer (Li-Po) battery pack contained within the hub, Figure 9.

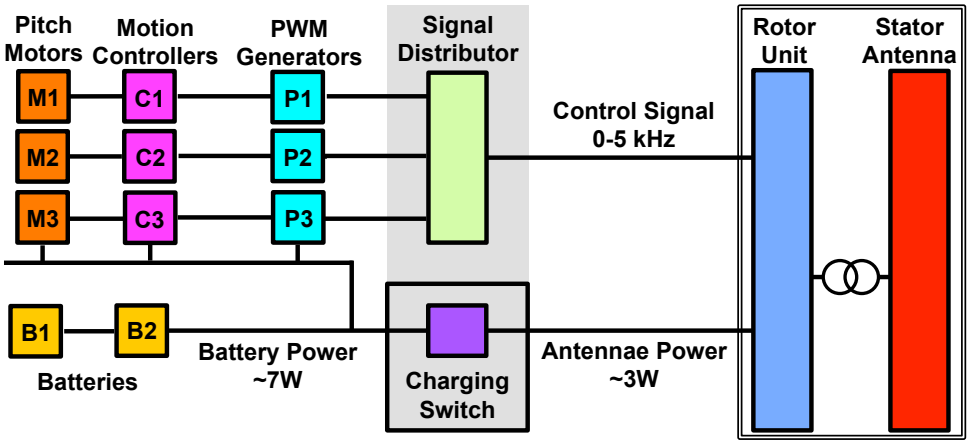

Figure 9: Schematic showing active switch that swaps powers between motors and batteries; state of switch is commanded by the control signal.

Continuous operation of the model turbine lasts approximately 90 seconds, including the time required for ramp-up of the turbine to design speed, traversing of the water channel by the carriage, and ramp-down of the turbine once the carriage has stopped; thus there is approximately 8 seconds of stable operation characterised by constant carriage velocity (±3.1%) and constant turbine rotational speed (±1.7%). At the design rotational speed, this 8 second window ensures 45-50 complete revolutions of the rotor, which is sufficient for statistically significant ensemble averaging. After completing a measurement, the inductive power transmission across the antennae is used to recharge the Li-Po batteries for 15 minutes.

4. ETH Zürich Wind Turbine Test Facility

4.1 Wind Turbine Test Facility

The experimental work of this project was carried out in ETH's Wind Turbine Test Facility (WEST facility), Figure 10. The facility consists of a water towing tank, with dimensions 40 m x 1 m x 1 m, through which the carriage-mounted sub-scale model wind turbine is drawn. Due to the use of water instead of air as the test medium, and the sub-scale turbine geometry, the Reynolds number, based on the mean chord and the optimal tip speed ratio of 6.28, is 1.5×10^5. As a comparison, if the same sized model were used in a wind tunnel, the Reynolds number would only be of the order of 10^4, whereas full-scale modern multi-megawatt wind turbines have Reynolds numbers of approximately 5.0×10^6. A carriage, Figure 10, moves along the water tank. By varying the carriage speed, it is possible to simulate different wind speeds. Upstream of the carriage is an active turbulence generator that generates specified turbulence levels in the inflow. A pump at the downstream end of the carriage supplies water flow to the active turbulence generator.

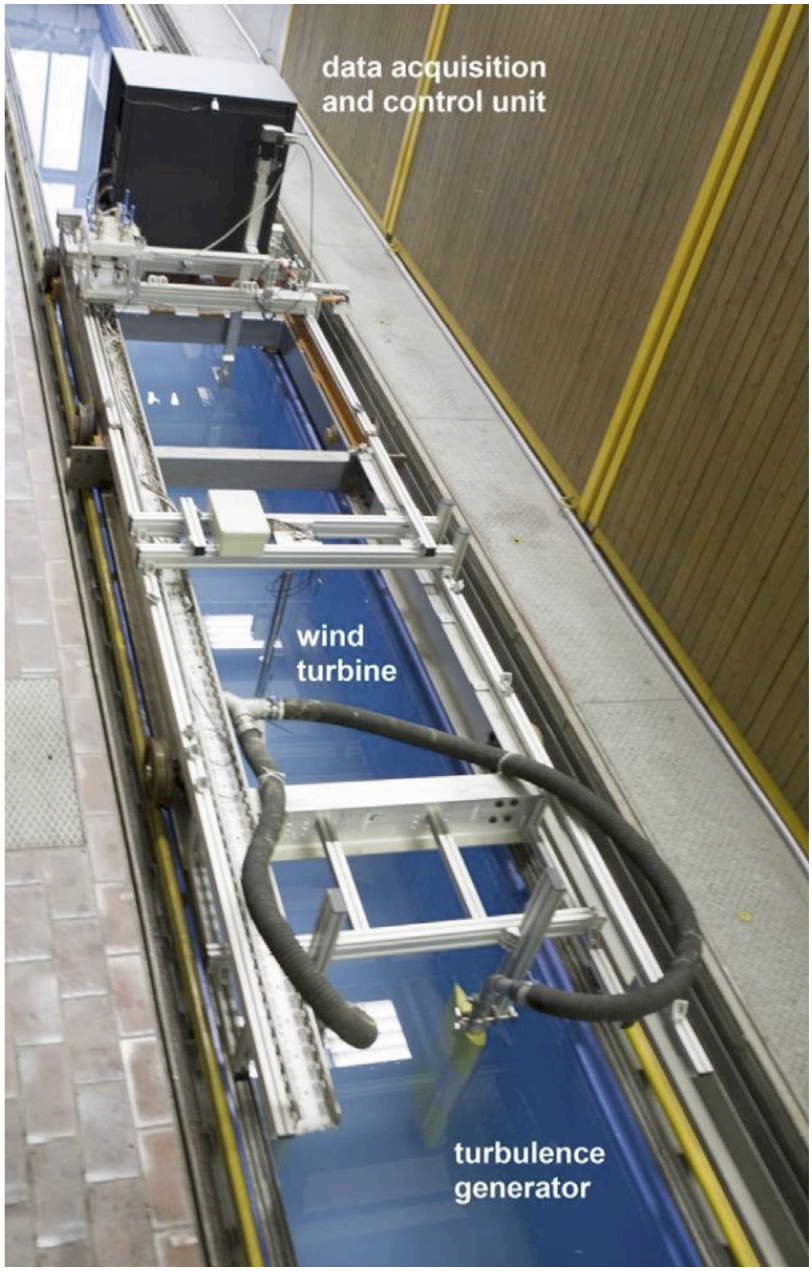

Figure 10: Bird's eye view of the ETH WEST Facility

4.2 Data acquisition and control system, and instrumentation

The data acquisition and control unit is mounted on the carriage allowing for control of the IPC system and the turbine rotational speed during testing, as well as time-resolved load measurements on the drive shaft of the turbine and on the tower. A full Wheatstone bridge on the driveshaft of the turbine isolates the shaft torque from the bending loads. The strain gauge configuration has been installed within the hollow titanium turbine driveshaft, together with an amplification circuit and an inductive telemetry system, which allows for time-resolved measurement of the shaft torque at a frequency of 10 kHz.

5. Effect of independent pitch control on power and performance

5.1 Algorithim for independent pitch control

In order to maximise the clearance between the tower and blade tip, modern multi-megawatt wind turbines are designed with rotor tilt; that is the axis of the rotor is inclined relative to the horizontal, typically in the range 5-10° depending on the manufacturer of the turbine and the design of the turbine. Rotor tilt results in an axial displacement of the blade tip (x), as shown in Figure 11.

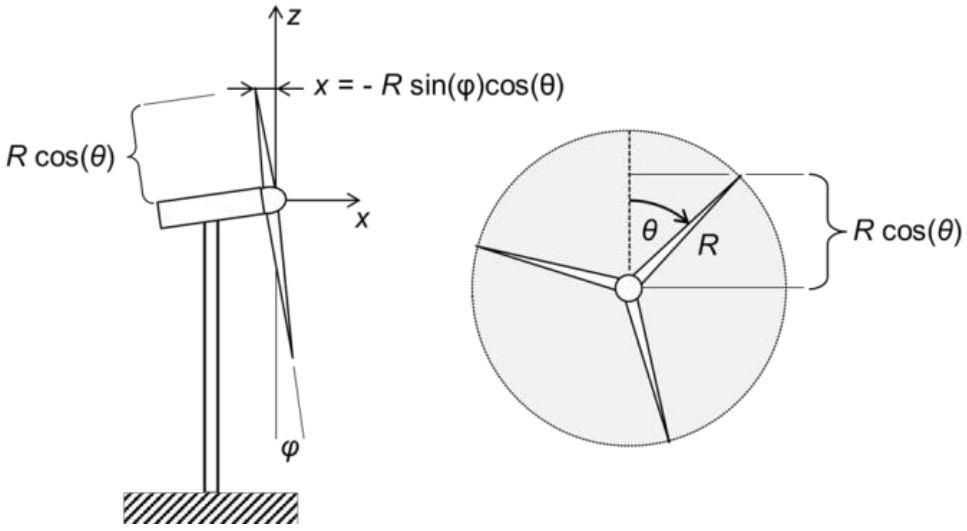

Figure 11: Schematic of rotor tilt showing the axial displacement of the blade tip, which results in an increased clearance of tower to blade tip.

The axial displacement of the blade tip is

$$x = -R\sin\varphi\cos\theta \quad (1)$$

and can be seen to be a function of the rotor radius (R), tilt angle (φ) and the azimuthal position of the rotor (θ). Revolution of the rotor, thus, causes the blade tip either to advance into the wind or conversely retreat away from the wind according to the relation:

$$\dot{x} = R\dot{\theta}\sin\varphi\sin\theta \quad (2)$$

dependent on the rotational speed of the turbine ($\dot{\theta}$). This advancement / retreat of the blade into / out of the wind causes a variation in the relative velocity that is seen by each blade section. Independent pitch control has been performed in this work by adding a corrective pitch adjustment (P_{IPC}) to the collective pitch angle (P_0) to compensate for the velocity variations that are induced by the rotor tilt effect. The corrective pitch adjustment (P_{IPC}) is linearly related to the rate of advancement / retreat ($\dot{x}$) which, upon integration, yields:

$$P_{IPC} = D\sin\theta \quad (3)$$

where the proportionality constant, D, encompasses the rotor radius (R) and turbine rotational speed ($\dot{\theta}$) with further dependence upon the rotor tilt (φ).

The velocity triangles shown in Figure 12 illustrate the effect of rotor tilt. A sinusoidal pitching scheme with a negative amplitude, on a clockwise-rotating downwind turbine ensures maximum pitch towards stall at an azimuthal position of θ = 90º (Figure 12a) and maximum pitch towards feather at an azimuthal position of θ = 270º (Figure 12b). At an azimuthal position of θ = 90º, Eq. 2 indicates that axial translation of the blade section occurs in the direction of the wind (the positive x-direction) reducing the relative velocity seen by the outboard blade sections. Conversely, at an azimuthal position of θ = 270º, axial translation of the blade section occurs against the direction of the wind (the negative x-direction) increasing the relative velocity seen by the blade. A negative sinusoidal pitching amplitude, thus, compensates for the velocity variation, induced by rotor tilt, by pitching the blade towards stall at an azimuthal position of θ = 90º, where the relative velocity is lowest, and pitching the blade towards feather at an azimuthal position of θ = 270º, where the relative velocity is highest.

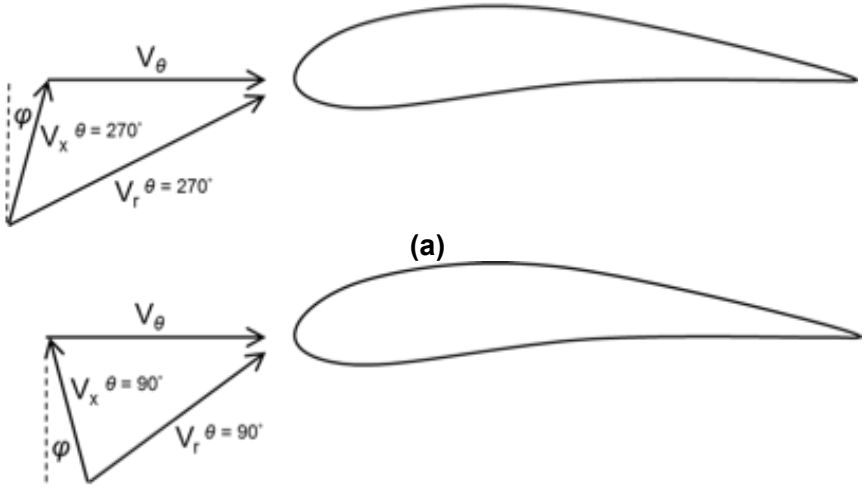

Figure 12: Velocity variations induced by rotor tilt: (a) velocity triangle at azimuthal position of θ = 90º; (b) velocity triangle at azimuthal position of θ = 270º.

All independent pitch control tests in this work have, thus, been performed with the sinusoidal pitching scheme, Eq. 3, in order to compensate for the velocity variations that are induced by rotor tilt.

5.2 Effect of independent pitch control

The impact of yaw on the power for the turbine with no pitch control is shown in Figure 13. The maximum power is achieved for the case of no yaw (0°), and the power decreases with increasing angles of yaw. An asymmetric trend can however be seen; that is, the power is higher for a positive yaw of 16°, 75% of the maximum power coefficient, whereas for a negative yaw of 16° the power is 62% of maximum power (13% lower than the power in the reciprocal positive yaw case).

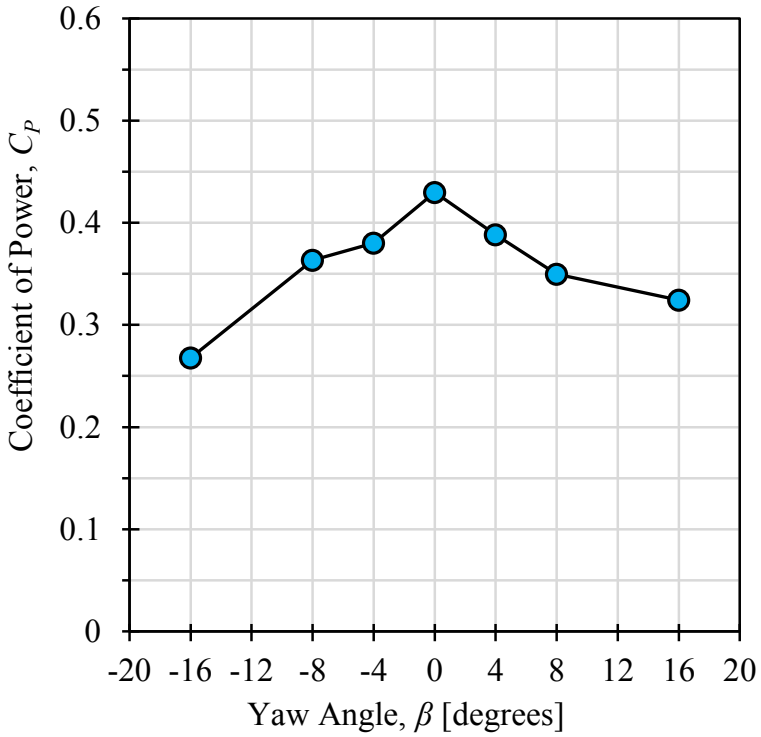

Figure 13: Effect of yaw angle on power for turbine with no pitch control.

The effect of individual pitch control (IPC) for the case of 0° yaw, as well ±16° yaw, with and without sinusoidal pitching are shown in Figure 14. Pitching amplitudes (*D*) of ±0.8°, ±1.6°, ±2.4° and ±3.2° are shown. The maximum power is achieved with a sinusoidal pitching amplitude (D) of -1.6° for all cases, with a decrease in power observed for pitching amplitudes of -2.4° and -3.2°. Positive pitching amplitudes also reduced power for all cases. The optimum pitching amplitude is thus observed to be independent of yaw.

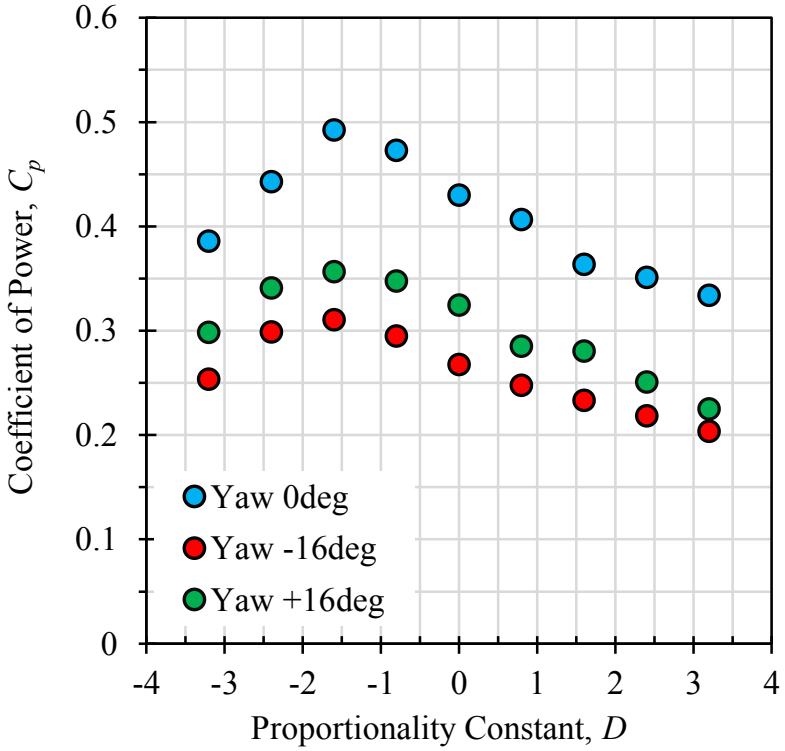

Figure 14: Effect of individual pitch control on power for turbine with no yaw and yaw = ±16°. The sinusoidal pitching amplitudes are ±0.8°, ±1.6°, ±2.4° and ±3.2°.

The trends in the effect of individual pitch control on power are mirrored in the effect on the thrust that is shown in Figure 15. The maximum thrust coincides with the maximum power for a pitching amplitude of -1.6° in all cases; thus, also for thrust the optimum pitching amplitude is independent of yaw. However, whereas the power is higher for the case of positive yaw of 16° compared with negative yaw of 16°, in the case of the thrust, for positive and negative yaw of 16°, the thrusts are comparable.

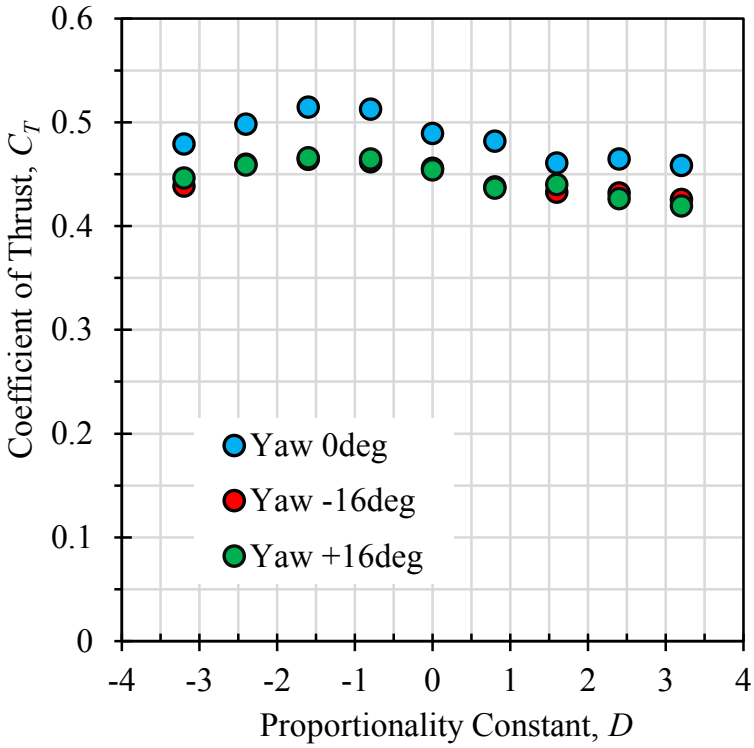

Figure 15: Effect of individual pitch control on thrust for turbine with no yaw and yaw = ±16°. The sinusoidal pitching amplitudes are ±0.8°, ±1.6°, ±2.4° and ±3.2°.

The effect of individual pitch control for the case of wind turbine operation at a rotor speed that is 10% less that the optimum TSR is shown in Figure 16 for the case of 0° yaw. It can be seen that the maximum power occurs for a pitching amplitude of -0.8°, which is different from the optimum amplitude of -1.6° at the design TSR. This dependence of the optimum pitching amplitude on the rotor speed is unsurprising in consideration of the velocity triangles that are shown in Figure 12. At an azimuthal position of θ = 90º, Eq. 2 indicates that axial translation of the blade section occurs in the direction of the wind (the positive x-direction) reducing the relative velocity over the outboard blade sections. Conversely, at an azimuthal position of θ = 270º, axial translation of the blade section occurs against the direction of the wind (the negative x-direction) increasing the relative velocity seen by the blade. A negative sinusoidal pitching amplitude, thus, compensates for the velocity variation, induced by rotor tilt, by pitching the blade towards stall at an azimuthal position of θ = 90º, where the relative velocity is lowest, and pitching the blade towards feather at an azimuthal position of θ = 270º, where the relative velocity is highest. Consequently, the power production is improved by the negative sinusoidal pitching scheme that compensates for the velocity variation induced by rotor tilt. The insensitivity of this pitching scheme to yaw supports the relationship between the sinusoidal pitching and rotor tilt, whereas the sensitivity to TSR can be explained by the dependency of the velocity variations on the axial translation of the blade which, in turn, depends upon the turbine rotational speed, as indicated by Eq. 2.

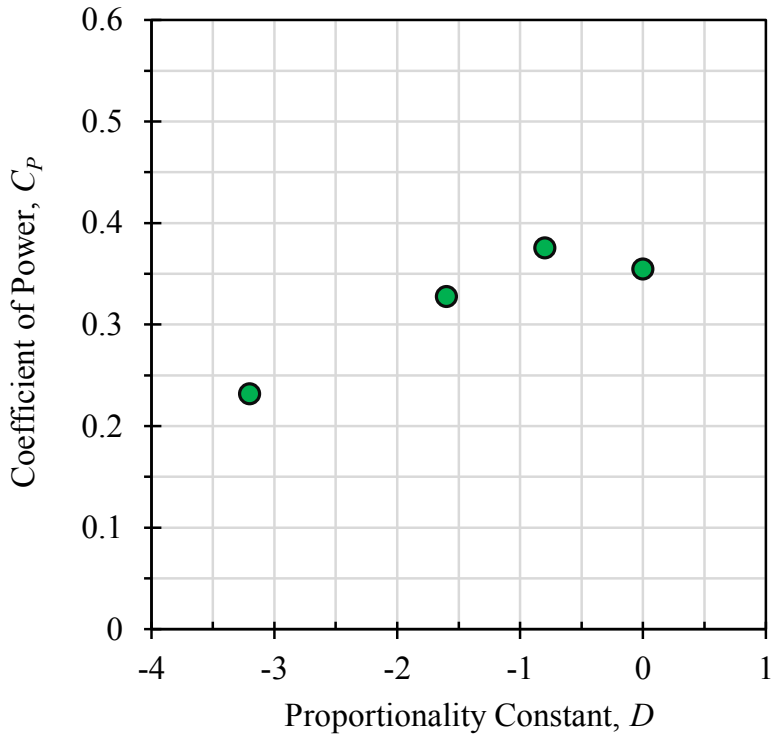

Figure 16: Effect of individual pitch control on power at off-design operation. The pitching amplitudes are 0°, 0.8°, 1.6°, and 3.2°, and yaw = 0°.

5.3 Effect of elevated turbulence on evolution of wakes

In prior work [8], the authors have examined the evolution of wakes in low freestream turbulence levels, of the order of 2%. In the present work, the evolution of wakes in elevated freestream turbulence levels, of the order of 10%, was measured. Figure 17 shows the wake that is measured four diameters downstream of the turbine. It can be seen that the distribution of velocity in not axisymmetric on account of the rotation of the work. The asymmetry in the velocity distribution is evident from the variation of the streamwise velocity in the wake across the horizontal span and vertical extent of the wake, as shown in Figure 18.

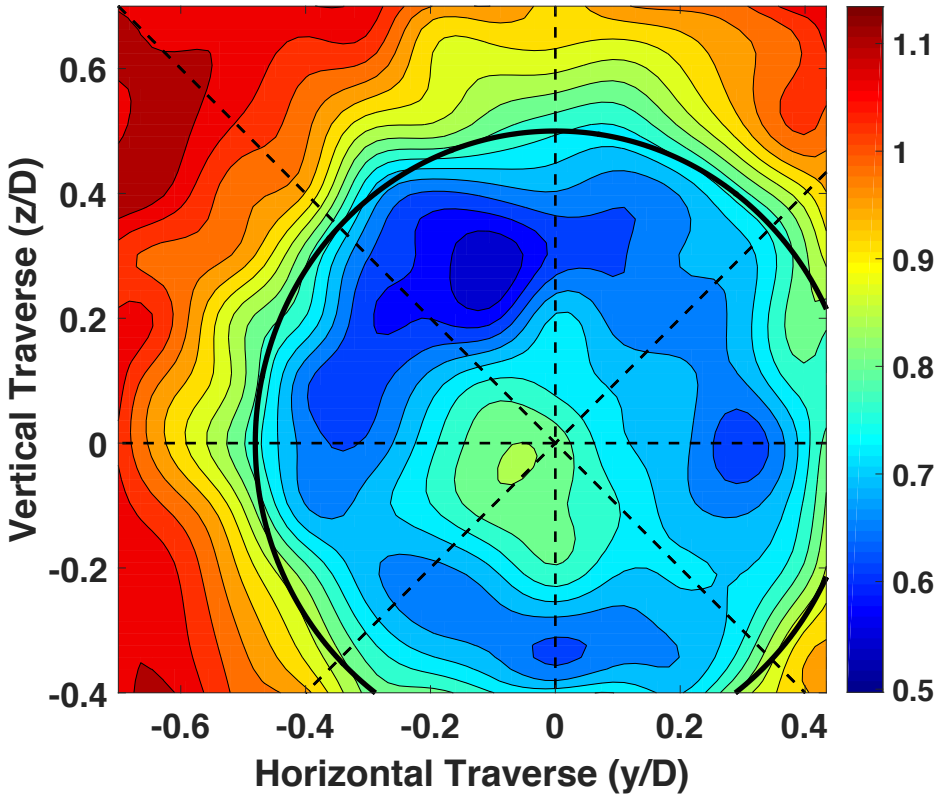

Figure 17: Wake measured four diameters downstream of turbine in elevated freestream turbulence. Yaw = 0°. The contours show the normalised streamwise velocity.

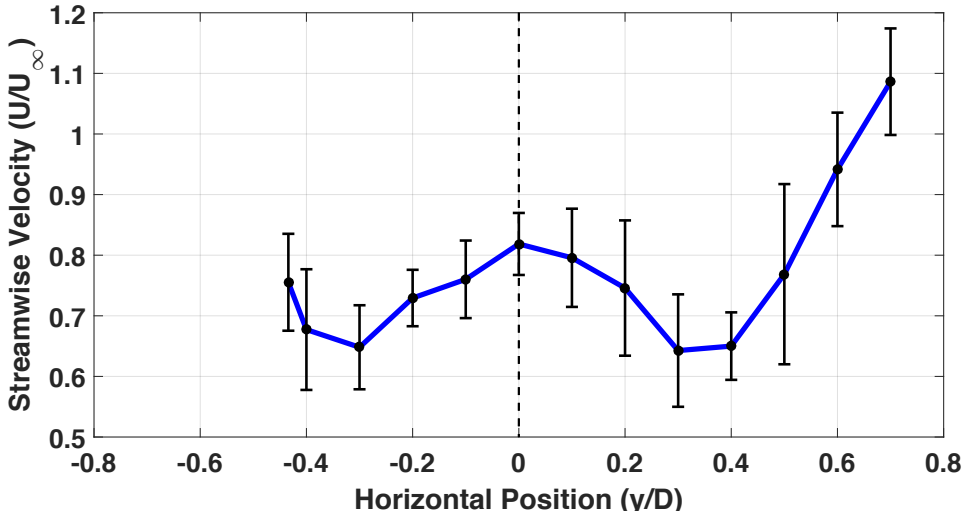

(a)

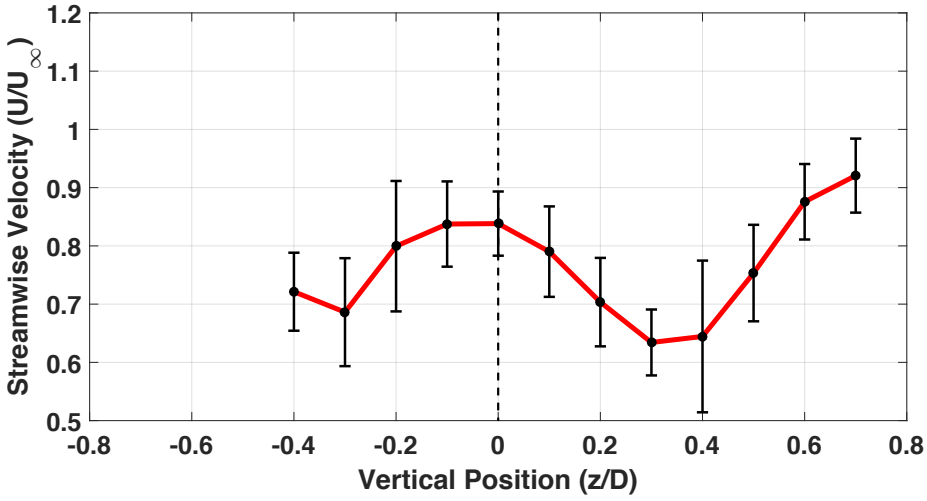

(b)

Figure 18: Distribution of streamwise velocity (a) across horizontal span of wake, and (b) across vertical extent of wake.

Figure 19 shows the effect of yaw on the structure of the wake. The measurements are again made four diameters downstream of the turbine, and the wake with no yaw is compared with the wake with yaw. It can be seen that asymmetry in the wake is increased with increasing yaw.

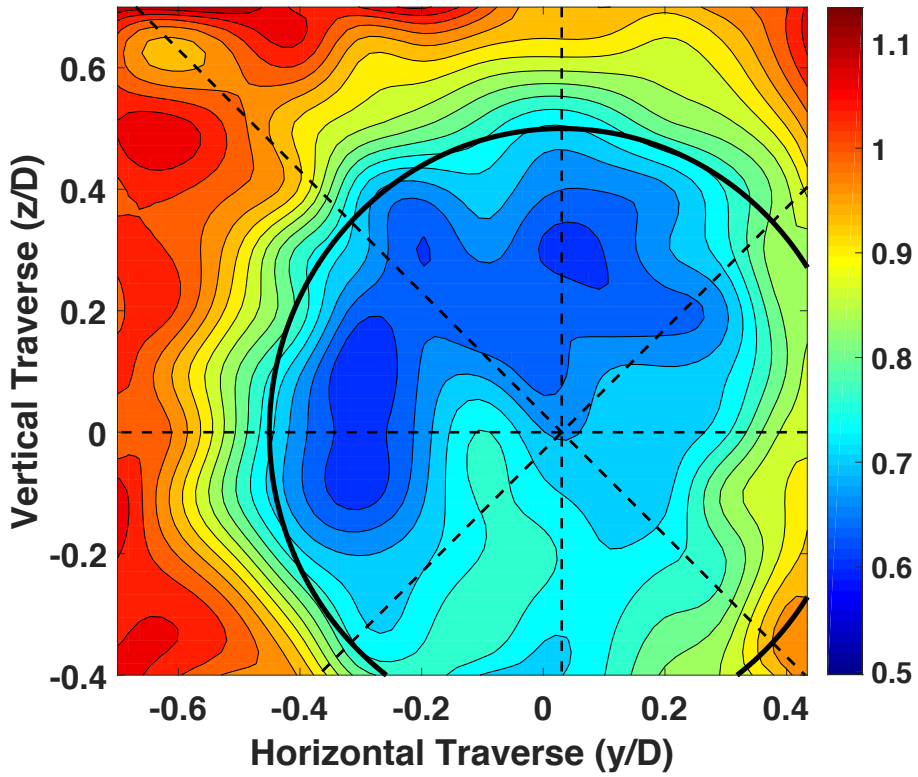

Figure 19: Wake measured four diameters downstream of turbine in elevated freestream turbulence. Yaw = 16°. The contours show the normalised streamwise velocity. The measured wake can be compared with the wake in zero yaw case that is

shown in Figure 17.

6. Conclusions

6.1 Concluding remarks

A scaled-model of modern, variable-speed, variable-pitch, multi-megawatt turbines that are representative of wind turbines recently installed in Switzerland, and that shall need to be installed to meet the goals of Switzerland's Energy Strategy 2050, has been designed, manufactured and installed in the ETH WEST Facility. The turbine model is equipped with independent pitch control mechanism, such that the pitch of each blade can be independently controlled. Furthermore, the drivetrain of the turbine model is designed such that the rotational speed of the turbine can be independent controlled. Thus, this unique scaled-model turbine has the essential characteristics of modern, variable-speed, variable-pitch, multi-megawatt turbines. To the knowledge of the authors, this is the first sub-scale model with independent pitch control that is used in a sub-scale model wind-turbine test facility.

Independent pitch control (IPC) based on sinusoidal pitching that is locked to the phase of the rotor rotation is demonstrated to achieve improvements in power:

– The optimum pitching amplitude for maximum power production is -1.6º for the case of 0º yaw, as well as ±16º yaw, indicating insensitivity to the yaw angle, with power increases between 10-16%.

– The power increase occurs because sinusoidal pitching, with a negative amplitude, compensates for the velocity variations induced by rotor tilt. The velocity variations occur because the tilt of the rotor axis causes each blade section to translate into / out of the wind during revolution of the rotor.

– The optimal pitching amplitude for peak power production, thus, does depend on the rotational speed of the turbine / the tip speed ratio (TSR).

The impact of the elevated turbulence on the evolution of the wake was experimentally assessed. It was observed that the wake is asymmetric, and this asymmetry is attributed to rotation of the wake.

6.2 Outlook

In prior work [8], the The overall goal of this project was to quantify the effects of elevated turbulence levels on the loads on wind turbines. In order to accomplish this it was necessary to design and manufacture (i) a scaled-model of a multi-megawatt wind turbine, and (ii) to design and manufacture an independent pitch control system for the model. The second task proved to be quite formidable, and several mechanical, electrical and electronic setbacks were encountered in the development of the independent pitch control system. While this resulted in delays to the schedule, a unique model, which to the authors' knowledge, is the first such sub-scale model with independent pitch control has been accomplished. Nevertheless a comprehensive set of load measurements in elevated turbulence were not accomplished; it is planned to accomplish these measurements in a following project.

7. Academic value added

A PhD student and several mechanical engineering Masters studens were involved in this project. In particular, this project attracted the Masters students to the many opportunities in the field related to the decarbonisation of the energy system. A Masters student thesis ("Pitch-Actuated Stability of Floating Downwind Wind Turbines.") and a Semester Project ("Blade Pitch Conrol Mechanism for Experimental Wind Turbine Model.") were outcomes from the work of this project. Further a PhD thesis project was also undertaken. Also, the world's leading expert in pitch control for wind turbines, Dr. Bossanyi, Senior Principal Researcher – Renewable, DNV GL (formerly Garrad Hassan), visited ETH after experimental results using the reinforced pitch mechanism were obtained. Dr. Bossanyi is world reknowned also as the principal developer of the commercially successful and wide-used aeroelastic simulation code, *Bladed*, for prediction of wind turbine performance performance and loading. Dr. Bossanyi remarked that the ETH model is worldwide unique and the only such in which to his knowledge experimenatal results are obtained; in the wind industry the norm is to generate such insight using simulations which are now to be lacking experimental validation.

As the model turbine with IPC represents a worldwide unique capability, the value of the work accomplished at ETH, including in particular that accomplished in this work, has strenghtened ETH's position a global leader in the field. Indeed, within the context of the IEA Wind, ETH was invited to join other global wind energy thought leaders in formulating a *Grand Vision for Wind Energy* vision as part of the activities of a Topical Experts Meeting. Furthermore, ETH is has also participated as founding participant in the IEA Wind Task 40 that focuses on downwind turbine technologies. A key enabler to accomplishing low cost of wind-generated electricity using this downwind technology is use pitch control to manage performance and loads. Thus it is anticipated that ETH's model turbine with IPC, that has been developed in the present project, is a key element. Indeed, it is evident that through its activitivies in IEA Wind, ETH is enable to foster and develop international collaborations with other universities and research centers.

8. Links to industry

This project leveraged the strong industrial partnership that ETH has with Hitachi Ltd. of Japan. Indeed, ETH is the primary university technology development partner of Hitachi Ltd. As Hitachi Ltd is based in Japan that has complex terrain quite similar to the terrain of Switzerland, and Hitachi Ltd. is the world's leading commercial manufacturer of downwind turbines [9] this strong link to Hitachi Ltd. through the ETH-Hitachi project "Load Alleviation and Control of Floating Multi-Megawatt Downwind Turbines" enhanced this project. Specifically, through the ETH-Hitachi collaboration, ETH were able to discuss specific characterisitics of full-scale turbines that allowed that ETH could ensure that pitch mechanisim integrated into the model turbine is representative of that on a modern multi-megawatt turbine.

Also during the course of this project, several discussions and visits were made between ETH and two turbine manufacturers, Gamesa and Siemens. Specifically, Dr. Ruediger Knauf, CTO of Siemens Wind Power accompanied by technical staff from Siemens Wind Power visited ETH to explore possible projects. Also Dr. Chokani made presentations to Dr. Mauro Villanueva-Monzón, Technology Development Director and staff of theTechnology Directorate in Madrid to explore possible projects. During the course of these discussions, Gamesa and Siemens merged into the joint company Siemens Gamesa Renewable Energy SA. Thus, while no project could be concluded due transitions that took place during the merger, it is expected that a project will subsequently be developed.

This project focused on elevated turbulence levels. Thus the conditions simulated in the ETH WEST Facility were based on ETH's measurements of the atmospheric wind and wake flows in the Mont Crosin wind farm that is owned and operated by Juvent, a branch of BKW FMB Energie AG. ETH's measurements were conducted using ETH's windRoverII that is equipped with a 3D scanning LIDAR system.

9. References

[1] Njiri J.G. and Söffker D. (2016) State-of-the-art in wind turbine control: trends and challenges. Renewable and Sustainable Energy Reviews 60, 377-393.

[2] Bossanyi E.A. (2005) Further load reductions with individual pitch control. Wind Energy 8, 481-485.

[3] Bossanyi E.A. (2003). Individual blade pitch control for load reduction. Wind Energy 6, 119-128.

[4] Trudnowski D. and LeMieux D. (2002) Independent pitch control using rotor position feedback for wind-shear and gravity fatigue reduction in a wind turbine. Proceedings of the American Control Conference. Anchorage, Alaska. 8-10 May 2002.

[5] Wang N., Wright A.D. and Johnson K.E. (2016) Independent blade pitch controller design for a three-bladed turbine using disturbance accommodating control. American Control Conference. Boston, USA. 6-8 July 2017.

[6] Zhang Y., Chen Z., Cheng M. and Zhang J. (2011) Mitigation of fatigue loads using individual pitch control of wind turbines based on FAST. International Universities' Power Engineering Conference. Soest, Germany. 5-8 September 2011.

[7] Kress C., Chokani N., Abhari R.S. (2016) Passive minimisation of load fluctuations on downwind turbines. Renewable Energy 89, 543-551.

[8] Barber S., Chokani N., Abhari R.S. (2013) Effect of wake flow nonuniformity on wind turbine performance and aerodynamics. ASME Journal of Turbomachinery 135, 011012.

[9] Saeki M., Tobinaga I., Sugino J., Shiraishi T. (2014). Development of 5-MW offshore wind turbine and 2-MW floating offshore wind turbine technology. Hitachi Review, 63(7) 414-421.